Article:
Strother, P.K., Brasier, M.D., Wacey, D. et al. (3 more authors) (2021) A possible billion-year-old holozoan with differentiated multicellularity. Current Biology. ISSN 0960-9822

https://doi.org/10.1016/j.cub.2021.03.051

Report

Current Biology

A possible billion-year-old holozoan with differentiated multicellularity

Graphical abstract

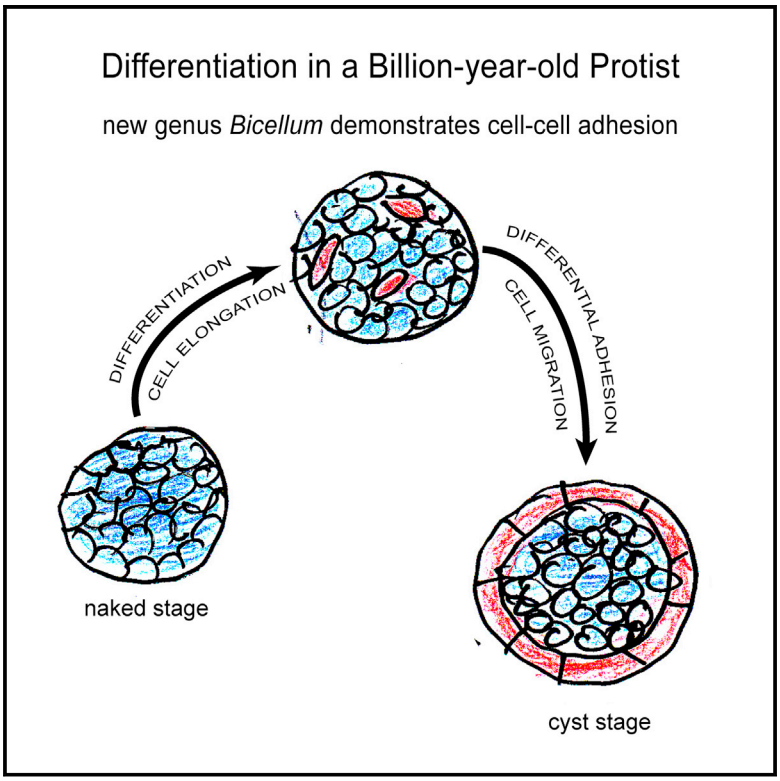

Authors

Paul K. Strother, Martin D. Brasier, David Wacey, Leslie Timpe, Martin Saunders, Charles H. Wellman

Correspondence

strother@bc.edu

In brief

Strother et al. describe life cycle morphogenesis in a new billion-year-old microfossil, which may provide clues to the evolutionary roots of embryonic development in animals.

Highlights

- The multicellular microfossil *Bicellum brasieri* possesses two distinct cell types
- 3D preservation in phosphate preserved different life cycle stages
- Differential adhesion may have contributed to cell segregation during morphogenesis
- This billion-year-old freshwater protist shows evidence of holozoan affinity

Strother et al., 2021, Current Biology *31*, 1–8
June 21, 2021
https://doi.org/10.1016/j.cub.2021.03.051

CellPress

Current Biology

CellPress
OPEN ACCESS

Report

A possible billion-year-old holozoan with differentiated multicellularity

Paul K. Strother,[1,7,*] Martin D. Brasier,[2,6] David Wacey,[3] Leslie Timpe,[4] Martin Saunders,[3] and Charles H. Wellman[5]
[1]Department of Earth & Environmental Sciences, Weston Observatory of Boston College, 381 Concord Road, Weston, MA 02493, USA
[2]Department of Earth Sciences, University of Oxford, South Parks Road, Oxford OX1 3AN, UK
[3]Centre for Microscopy, Characterisation and Analysis, The University of Western Australia, 35 Stirling Highway, Perth, WA 6009, Australia
[4]Department of Biology, San Francisco State University, San Francisco, CA 94132, USA
[5]Department of Animal & Plant Sciences, University of Sheffield, Alfred Denny Building, Western Bank, Sheffield S10 2TN, UK
[6]Deceased
[7]Lead contact
*Correspondence: strother@bc.edu
https://doi.org/10.1016/j.cub.2021.03.051

SUMMARY

Sediments of the Torridonian sequence of the Northwest Scottish Highlands contain a wide array of microfossils, documenting life in a non-marine setting a billion years ago (1 Ga).[1–4] Phosphate nodules from the Diabaig Formation at Loch Torridon preserve microorganisms with cellular-level fidelity,[5,6] allowing for partial reconstruction of the developmental stages of a new organism, *Bicellum brasieri* gen. et sp. nov. The mature form of *Bicellum* consists of a solid, spherical ball of tightly packed cells (a stereoblast) of isodiametric cells enclosed in a monolayer of elongated, sausage-shaped cells. However, two populations of naked stereoblasts show mixed cell shapes, which we infer to indicate incipient development of elongated cells that were migrating to the periphery of the cell mass. These simple morphogenetic movements could be explained by differential cell-cell adhesion.[7,8] In fact, the basic morphology of *Bicellum* is topologically similar to that of experimentally produced cell masses that were shown to spontaneously segregate into two distinct domains based on differential cadherin-based cell adhesion.[9] The lack of rigid cell walls in the stereoblast renders an algal affinity for *Bicellum* unlikely: its overall morphology is more consistent with a holozoan origin. Unicellular holozoans are known today to form multicellular stages within complex life cycles,[10–13] so the occurrence of such simple levels of transient multicellularity seen here is consistent with a holozoan affinity. Regardless of precise phylogenetic placement, these fossils demonstrate simple cell differentiation and morphogenic processes that are similar to those seen in some metazoans today.

RESULTS

Butterfield[14] has pointed out that multicellular organisms in pre-Ediacaran age deposits were likely to have left behind ontogenetic stages in the fossil record. We have examined about 50 petrographic thin sections of phosphatic lenses in the Diabaig Formation (ca. 1 Ga) that preserve populations of benthic and planktic organisms trapped in former lake bottom sediments (Figures 1A–1D). These include unicells and cell clusters of various kinds, some of which have been documented previously.[1,2,6,15] In several thin sections, we observed cell clusters that are composed of aggregations of two distinct cell types, indicating a condition that constitutes a step toward complex multicellularity *sensu* Knoll.[16] Further investigation revealed a second set of cell clusters that appeared very similar in size and form but that lacked the fully differentiated second cell type. Here, we describe these interesting fossils and show intermediate morphologies that are consistent with an ontogenetic series driven by a differential cell-adhesion model.

The morphology of the new multicellular organism consists of a spheroidal mass of mutually adpressed cells enclosed by a peripheral layer of elongate, sausage-shaped cells. The interior cell mass forms a stereoblast (Figures 2A–2C, 2F, 2H, 2J, and S1–S3) of roughly isodiametric cells that average ~2.5 μm in diameter (Table S1). Exceptional preservation in calcium phosphate (francolite) and authigenic clay minerals[5] (Figure S3) retains intracellular biological features that, in this case, consist of a single dense, organic "spot" (Figures 2A and 2C, arrows). In well-preserved specimens, such inclusions occur in about half of the interior cells. These might represent preserved nuclei, but we consider that, more likely, they are the condensed remains of the entirety of the cytoplasmic cell content.[6] The cells of the stereoblast retain mutually compressed walls, so that the original multicellular topology, including Y-shaped junctions[17] (Figures 2B and 2C, circles), is retained. There is no evidence that these interior cells possessed rigid cell walls, because the shape of each cell is established by mutual compression with adjacent cells. This indicates the likelihood that individual cells were bounded by just a cell membrane or a thin, non-rigid cell wall. A carbon map of a specimen from an ultrathin section (Figures 2J and S3) also shows very thin interior walls as compared with the exterior cell layer. Although it is not

Please cite this article in press as: Strother et al., A possible billion-year-old holozoan with differentiated multicellularity, Current Biology (2021), https://doi.org/10.1016/j.cub.2021.03.051

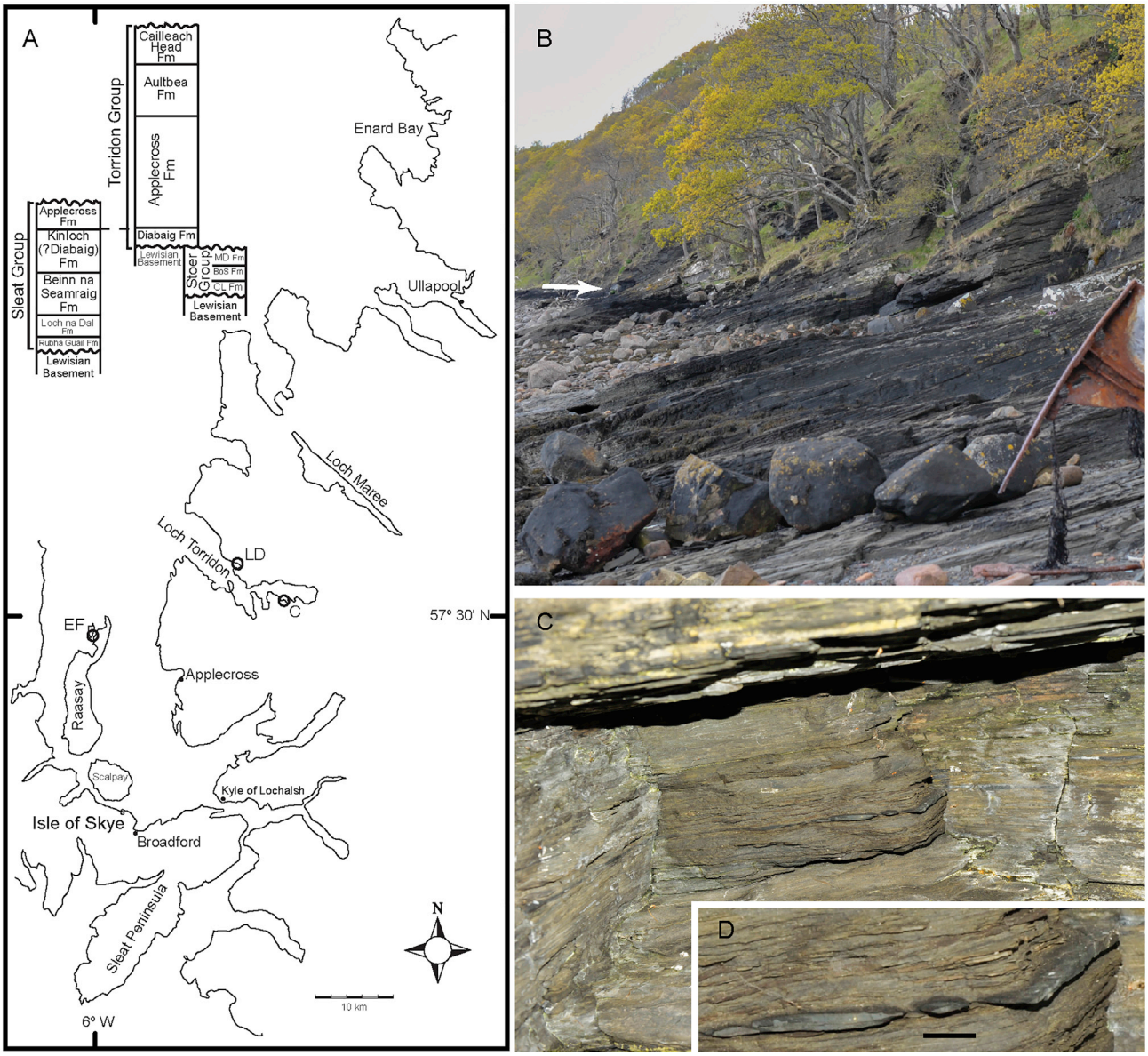

Figure 1. Location map and geological section at Lower Diabaig

(A) The location of studied materials mentioned in this report is indicated. LD, Lower Diabaig; CH, Cailleach Head; EF, Eilean Fladday; B, section near Balgy. (B) View of Diabaig Formation type section along the north shore of Loch Diabaig at the village of Lower Diabaig. The arrow marks the sample site. (C and D) View of dark shales (C) with lenticular, bedded phosphatic nodules *in situ* (D). Scale bar in (D), 5 cm.

possible to completely rule out that each of the interior cells possessed a thin, flexible cell wall, we found no examples of cells that possessed interior membranes that might have pulled away from any such cell wall. This is not the case for various other isolated cells of different organisms found throughout the Diabaig phosphates in which multiple concentric layers are apparent and in which true cell walls are quite evident.[6]

The outermost cell layer consists of thicker walled, sausage-shaped (elongate) cells, which form an enclosing layer that is unmistakably distinct from the isodiametric cells found in the interior stereoblast (Figures 2A, 2B, 2D–2K, and S1–S3). The elongate cells that form the peripheral layer are around 1.5 to 2 μm in diameter and generally about 3 to 4 times that in length, although, in some cases, they can be much longer (e.g., Figure 2K). The average width-to-length ratio for a set of 6 specimens was 0.28 (Table S1). The elongate shape is best demonstrated in surficial focus, as seen in Figures 2E–2G, 2I, and 2K (see also Figures S1–S3). Here, these cells crowd together to form what appears to be a rigid, outer spherical shell. The peripheral cells often occur in sets of 4 or more adjacent cells that are positioned parallel to each other (Figures 2F, 2G, 2I, 2K, and S1–S3), creating a tiled arrangement of sets of parallel cells, or, in some cases, covering the entire surface of the stereoblast in parallel-aligned, elongate cells (Figure 2K).

Please cite this article in press as: Strother et al., A possible billion-year-old holozoan with differentiated multicellularity, Current Biology (2021), https://doi.org/10.1016/j.cub.2021.03.051

CellPress
OPEN ACCESS

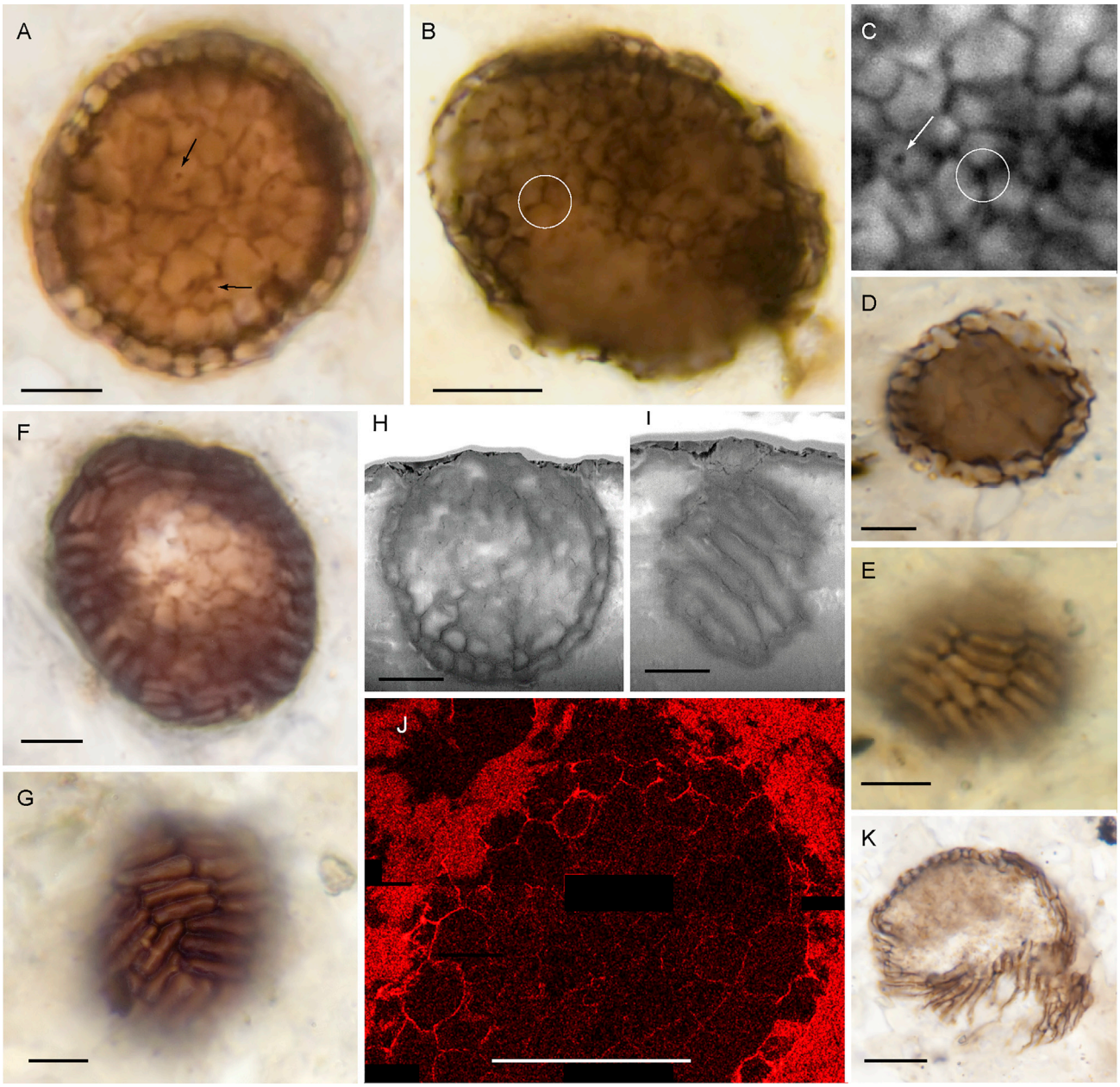

Figure 2. *Bicellum Brasieri* in mature form

All specimens were preserved in petrographic thin sections from the Diabaig Formation stratotype, Lower Diabaig, Scotland, UK. Scale bars in (A)–(J), 5 μm; scale bar in (K), 10 μm.

(A) *Bicellum brasieri* n. g. n. sp. holotype specimen. Arrows indicate condensed, intracellular organic "spots" Sample TS09-1.

(B) *Bicellum brasieri* n. g. n. sp. paratype. Larger ellipsoidal specimen with incomplete preservation in the interior. Circle indicates an example of a Y-shaped junction. Sample TS09-1.

(C) Enlargement of holotype specimen showing typical "Y" junctions (circle) and a condensed intra-cellular "spot." Total field of view is 10 μm.

(D) Specimen in equatorial view in which the interior cells are only very faintly preserved. Sample TS09-2.

(E) Surface view of specimen in (D), showing the tiled sets of parallel-aligned elongate cells.

(F) Specimen in sub-equatorial optical section showing elongate exterior cells in surface view and the thinner walled isodiametric cells of the interior stereoblast. Sample TS09-2.

(G) Surface view of specimen in (F), showing the tiled pattern of sets of elongate cells.

(H) Scanning electron microscopy (SEM) image of an *in situ* milled medial section through *B. brasieri*. Sample TOR11-108.

(I) SEM image of a milled tangential section of same specimen as in (H). Note that, here, the cells of the surface layer are quite elongate.

(legend continued on next page)

Please cite this article in press as: Strother et al., A possible billion-year-old holozoan with differentiated multicellularity, Current Biology (2021), https://doi.org/10.1016/j.cub.2021.03.051

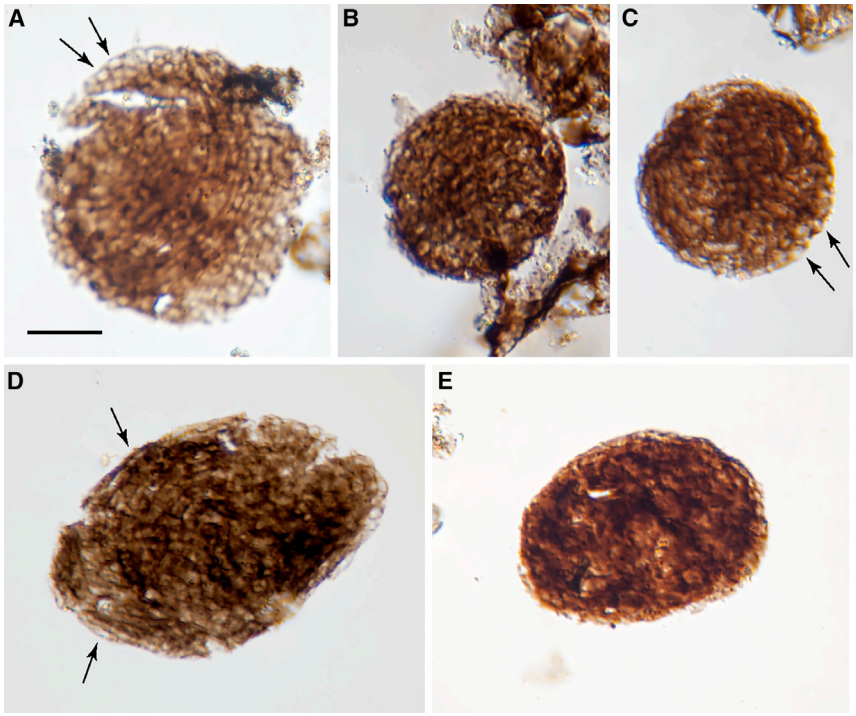

Figure 3. Examples of the distributed (palynological) form

All figured specimens are from sample TOR11-9, Eilean Fladday, Scotland, UK. Scale bar, 10 μm for all images.

(A) Spherical form characterized by circular cross sections in an epidermal layer (arrows).

(B) Typical specimen without clearly demarked cell outlines.

(C) Spherical specimen showing circular cross-sections in the epidermal layer (arrows).

(D) Somewhat larger ellipsoidal specimen. Here, arrows indicate more elongated cells of the epidermal layer. Note that the right-hand margin indicates epidermal cells in circular cross-section.

(E) Oblate specimen without clear cellular structural interior.

See also related size data in Table S2.

In medial cross-section, the peripheral cell layer is shown to be one cell in thickness (Figures 2A, 2B, 2D, 2H, 2J, and S1–S3). In light microscopy (LM), the walls of these outer cells appear darker than those of the stereoblast, indicating a thicker cell wall, distinct from those of the interior cells. This is seen in the holotype (Figure 2A) and in many of the other illustrated specimens (e.g., Figures 2D, 2H, 2J, S1, and S2). This is also somewhat evident in the carbon map in Figure 2J, although in this specimen, the carbon signal from the cells of the epidermal layer is masked somewhat by the carbon signal from the enclosing francolite (see also Figures S3E and S3F). The cells of the peripheral layer never show an interior "spot" like many cells of the stereoblast, indicating a persistent taphonomic difference in the two cell types, or perhaps loss of the protoplast at maturity in the epidermal cells, as, under LM, their interiors are more transparent that those of the interior stereoblast. Many specimens show some degree of cell loss within the stereoblast as a whole. This can be seen in medial sections of Figures 2B and 2D, where parts of the interior are missing well-preserved cells (see also Figure S1). Overall, this arrangement of two distinct cell types forming a spherical organism has not been previously described in the fossil record and is formalized here as *Bicellum brasieri* Strother & Wellman gen. et sp. nov.

The structural details used to describe *Bicellum* exist because of the unique qualities of cellular and sub-cellular preservation provided by phosphate and authigenic clay mineralization.[5,6] The taxonomic richness that characterizes the Torridonian lake deposits, however, is recorded primarily in palynological preparations of fine-grained siliciclastic rocks that yield organic-walled microfossils (OWMs).[1] An OWM comparable to *Bicellum* was also recovered in palynological strew mounts, but, as documented in Figure 3, its appearance as a flattened, dispersed OWM is somewhat different than its 3D form. Here, the wall is characterized by marginal circular structures (arrows in Figures 3A, 3C, and 3D), which correspond to cross-sectional views of the elongated cell peripheral layer. The average diameter (28.5 μm; Table S2) and ovoid (Figures 3D and 3E) to circular (Figures 3A–3C) shape are similar to the 3-dimensional form, but the interior stereoblast is not structurally preserved in the dispersed form, nor is the cellular nature of the peripheral layer readily apparent. In spite of these preservational differences, *Bicellum*, in its dispersed form, has now been recognized from 11 sample localities found throughout the Torridonian sequence (Table S2).

Tightly bound, spherical cell clusters found in association with *B. brasieri* fall outside the prescribed complex morphology for the species as presented here. These multicellular cell clusters consist of naked stereoblasts without an enclosing wall or cell layer. They are most commonly quite spherical (Figures 4A–4E), although some larger, ellipsoidal specimens have also been found (Figure 4F). The cells that compose each mass are tightly adpressed without intervening spaces; indeed, many exhibit straight lines of contact and clear 120° (Y-shaped) junctions where three cells meet. They are generally isodiametric, with diameters of 2 to 3 μm. The closeness of the cells indicates the originally cohesive nature of these cell masses; they appear as if they were tightly pressed together in life. The lack of intervening space also indicates that, in life, these cells did not possess rigid cell walls; if present, the cell walls clearly had a

(J) *B. brasieri* transmission electron microscopy-energy dispersive X-ray spectroscopy (TEM-EDS) elemental map of carbon revealing the thicker walled outer layer of sausage-shaped cells compared with the interior cells that have thin to partially absent membranes. Sample TOR11-108.

(K) Larger, fragmented specimen of *B. brasieri* showing surficial cells in transverse and tangential sections. Note the elongate nature of the tangential cells and the lack of clearly delineated interior cells. Sample TS09-1, Diabaig Formation stratotype, Lower Diabaig, Scotland, UK.

See also Figures S1–S3 for additional examples and Table S1 for related cell size data.

Please cite this article in press as: Strother et al., A possible billion-year-old holozoan with differentiated multicellularity, Current Biology (2021), https://doi.org/10.1016/j.cub.2021.03.051

CellPress
OPEN ACCESS

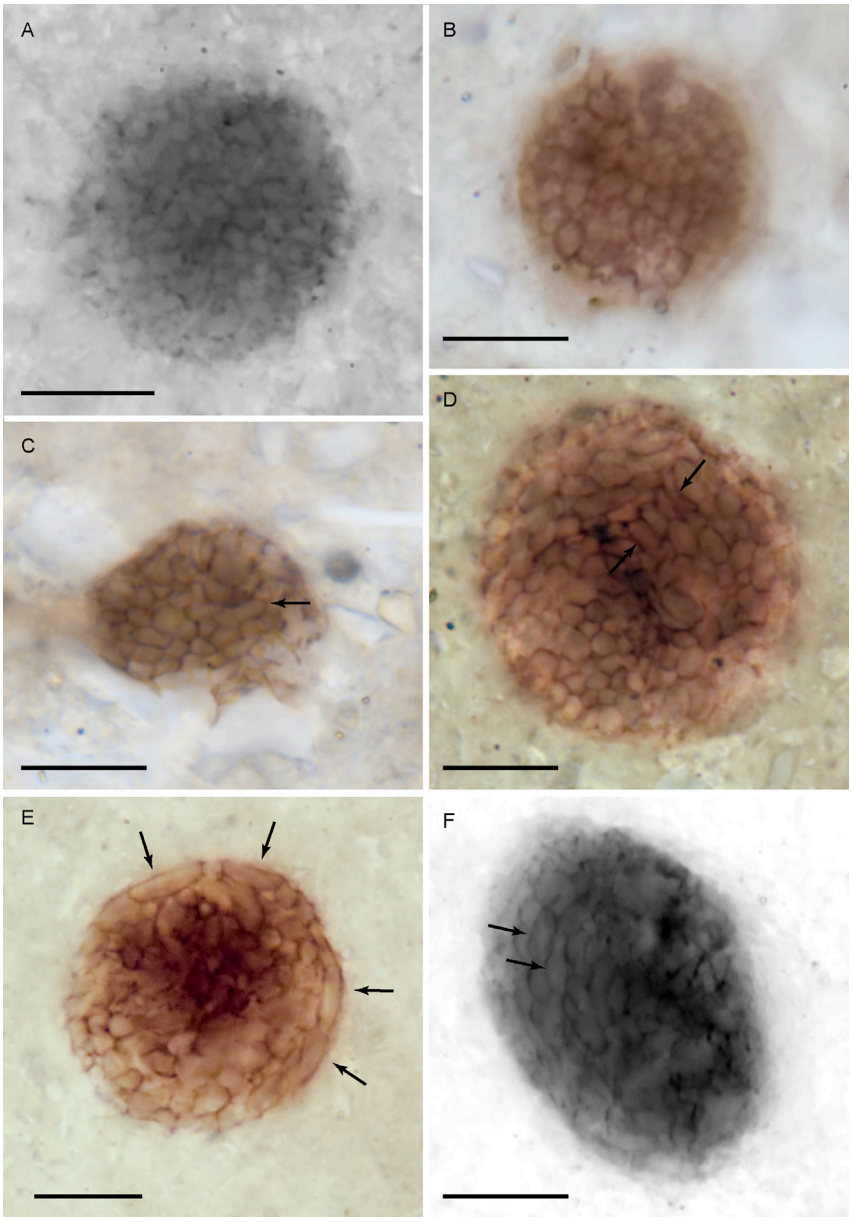

Figure 4. Naked stereoblasts

Except where noted, all specimens are from sample TOR11-108, Diabaig Formation stratotype, Lower Diabaig, Scotland, UK. Scale bar, 10 μm.

(A) Naked stereoblast of mutually adpressed isodiametric cells. Note the lack of a discrete outer layer of cells.

(B) Another example of a simple ball of isodiametric cells amassed together to form a naked stereoblast. Sample TS09-1, Diabaig Formation stratotype, Lower Diabaig, Scotland, UK.

(C) This somewhat smaller specimen shows a single elongate cell (arrow) in the midst of a solid mass of isodiametric cells. Sample TS09-2, Diabaig Formation stratotype, Lower Diabaig, Scotland, UK.

(D) Naked stereoblast with an admixture of elongate and isodiametric cells. There is a row of adjacent elongate cells (between arrows) in the middle of the cell mass, but cells at the margin are isodiametric in shape.

(E) Here, some elongate cells (arrows) now appear at the periphery of the cell mass, although a clearly distinct epidermal layer has yet to become established. Note that there is no apparent distinction between the cell walls of either cell type.

(F) This ellipsoidal specimen, which is cut in a subtangential section, shows substantial alignment of sausage-shaped cell types (arrows).

degree of plasticity. The adjoining cell walls are thin, never thickened like those in the peripherical cell layer of *B. brasieri*.

These free, spherical cell masses (Figures 4A and 4B) are indistinguishable from the stereoblasts that characterize the interior cells of *B. brasieri*. After examination, it became apparent that some of these masses occasionally included elongate cells, unlike the enclosed stereoblasts described earlier. The incomplete cell mass in Figure 4C contains only one such elongate cell (indicated by an arrow) in the midst of what are generally isodiametric cells. Figure 4D illustrates another example photographed in median optical section. Here, embedded among generally isodiametric cells, is a single row of elongate cells (between arrows). This specimen also contains a few additional isolated, individual, elongate cells scattered through the cell mass. Another specimen photographed in median section (Figure 4E), shows at least four elongate cells (indicated by arrows), which are now located at the periphery of the largely isodiametric cell mass. Here, these elongate cells appear to constitute part of a single circumferential layer, one cell in thickness, that surrounds the cell mass; however, the individual cells that make up this layer have thinner walls, matching those of all the interior cells of the stereoblast, and not thickened as seen in the peripheral layer of *B. brasieri*. The cell mass in Figure 4F appears somewhat even more organized, with several rows of nascent elongate cells preserved (indicated by arrows).

Although these cell clusters are nearly perfectly spherical in overall shape, the positions of individual cells within the clusters does not appear determinate: these cells do not appear to have retained a geometry based on fixed patterns of cell divisions. Cells capable of moving relative to each other, exhibiting liquid-like behavior, will spontaneously form spheres in response to minimizing overall surface tension.[18] Thus, on strictly morphological grounds, we infer that these fossils were originally aggregates of somewhat cohesive cells exhibiting liquid-like behavior.[19,20] Living cells aggregated in this way form the underlying basis of the differential adhesion hypothesis (DAH), which posits that cohesive cell aggregates are capable of self-differentiation when cell-cell cohesion varies between sets of cells.[8]

DISCUSSION

In spite of its simple morphology, the characterization of the *Bicellum* stereoblast, combined with an understanding of its

Please cite this article in press as: Strother et al., A possible billion-year-old holozoan with differentiated multicellularity, Current Biology (2021), https://doi.org/10.1016/j.cub.2021.03.051

dynamic assembly into a differentiated condition of two distinct cell aggregations, provides clues as to its systematic placement. It seems reasonable to assume that *Bicellum* falls within one of the lineages leading to one of the six clades that possess complex multicellularity today: animals, plants, florideophyte algae, brown algae, ascomycete fungi, and basidiomycete fungi.[16] The precise dynamics of how *Bicellum* attained its initial multicellular state has yet to be determined. In broad terms, this would have been through palintomy, aggregative assembly, or cellularization of a coenobium (syncytium). If the initial multicellular condition of *Bicellum* occurred through successive mitotic divisions, then we would expect to find cell clusters of similar overall size, exhibiting combinations of 2^n cells, as is the case, for example, in the embryo-like fossils of the Doushantuo phosphates. Although it is the case that many different kinds of cell clusters have been found in the same thin sections that contain *Bicellum*, no such palintomic sequence has yet been recognized. This indicates that the multicellular condition in *Bicellum* more likely occurred either through cell aggregation or through the cellularization of either a syncytium or a coenobium. Since these non-palintomic forms of multicellularity are also somewhat limited in their distribution within extant protist groups, they provide a means of limiting the potential placement of *Bicellum*. Other than in the opisthokonts, aggregative multicellularity occurs in the amoebozan, *Dictyostelium*, three SAR supergroup genera (*Sorogena*, *Sorodiplophrys*, and *Guttulinopsis*),[21] and also some labyrinthulids[22] and the Excavate *Acrasis*,[22] none of which are a morphological match with *Bicellum*. Formation of syncytia and/or coenobia occurs in the Archaeplastida and in all holozoan groups, with the exception of the choanoflagellates[13,22] and the Filasterea, which do show aggregative multicellularity.[23] However, the multicellular condition, as exhibited in the *Bicellum* stereoblast—that is, Y-shaped cell junctions and lack of fixed, or determinate, cell placement—indicates that these cells probably lacked rigid cell walls. This eliminates both cyanobacteria and the eukaryotic chlorophyte algae as likely homologs, because multicellular form in these taxa is strongly influenced by their possession of rigid cell walls.[17] This is also the case for comparison with the florideophyte red algae, which possess cellulosic cell walls and are fundamentally of filamentous or pseudoparenchymatous thallus organization. In addition, the red algae are predominantly marine in their habitat distribution,[24] as are the laminarian brown algae.[25] Y-shaped junctions in fossilized cell masses have most often been associated with tissue-grade multicellularity that is found in animals,[17,26–28] and this condition has been argued as a reason for considering many of the embryo-like fossils of the Doushantuo Formation to be related to animal (Holozoan) lineages rather than Archeoplastida.[17] Thus, in terms of its multicellular condition, *B. brasieri* seems to be most closely associated with early-branching holozoan groups, especially Ichthyosporea and the Pluriformea (Corallochytrea) clade.[13,29] These groups are all unicellular protists with a multicellular stage in their life cycle, typically occurring in the form of a spherical cell mass.[30]

The Precambrian occurrence of holozoans is documented in the well-known "embryo-like" fossils of the Doushantuo Formation, in spite of uncertainty as to their exact phylogenetic placement with respect to the Metazoa.[31–33] The Doushantuo fossils are found in considerably younger (ca. 600 Ma) deposits that are entirely marine in origin as compared with the billion-year-old lacustrine settings of the Torridonian.[34] Early-branching holozoan clades are not exclusively marine, however. Phylotypes of Ichthyosporea are found in freshwater and terrestrial settings today,[35] and the recently described filasterean, *Pigoraptor*, was isolated from nonmarine settings, as was *Syssomonas*, one of two genera in the recently proposed holozoan clade, Pluriformea.[13] Other Ichthyosporea and Filasterea, including species previously considered to be exclusively marine, have been detected in freshwater fluvial settings using environmental metabarcoding.[36] As to their antiquity, the existence of fossil holozoans by 1.0 Ga is perhaps not unexpected, given a reasonable estimate of the branch point between an ichthyosporean plus filasterean clade and the rest of the holozoan lineage at around 1,100 Ma,[37] although there is considerable uncertainty as to this date, based on molecular clock data.[38]

Phylogenomic investigations of metazoan origins have begun to assemble a picture of protistan gene regulatory networks that were later re-purposed during the evolution of the first Metazoa.[12,39,40] Intriguingly, various genes associated with cell-cell adhesion appear to be quite ancient, including the discovery that three cadherin families, (lefftyrin, coherin, and hedgling) were present in the last common ancestor between the choanoflagellates and the Metazoa.[41] Some core components of the integrin-mediated complex may predate even the initial evolutionary divergence in the Opisthokonta.[42]

Steinberg's differential adhesion hypothesis proposes that, for cases in which cell aggregates display liquid-like behavior, it is the strength of cell-cell adhesions that determines the overall form of the structure.[7,8] The dynamics of cell-cell segregation seen in *Bicellum* are compatible with that of a differential adhesion model in which the isodiametric cells adhere more strongly to each other than they adhere to the nascent elongate cells. This difference in cell-cell adhesion strengths is expected to give rise to a structure with an inner ball of isodiametric cells surrounded by a layer of elongated cells.[9,43,44] This mature stage then functioned as a cyst, which manifests as the more widely distributed form seen in Figure 3.

Although we are uncertain as to the molecular structure of the cell attachment apparatus in *Bicellum*, the reasons for differential adhesion are potentially simple. Foty and Steinberg[9] manipulated cadherin levels in cultured cells, showing that changing the expression level of that single protein was able to produce structures with an inner cell ball of strongly adhering cells surrounded by a cortex of more weakly adhering ones. However, even without a change in protein expression, an increase in surface area of the elongate cells, compared with that of the isodiametric cells, would reduce the surface density of adhesion molecules, leading to weaker adhesion between elongate and isodiametric cells. Whatever the mechanism, *Bicellum* does show that differentiation and morphogenesis occurred in the life cycles of freshwater protists as long as a billion years ago. This early example of complex multicellularity adds to a nascent body of evidence indicating the importance of selection in terrestrial settings during late Mesoproterozoic to early Neoproterozoic time.[4,45–47] Indeed, if *Bicellum* does belong to the clade Holozoa, as we suspect, it would provide support for recent models proposing Mesoproterozoic eukaryotic crown group origins,[48,49] and it could prove to be a key fossil clue in an ongoing

debate on the importance of oxygen in the origin and rise of animals.[50]

STAR★METHODS

Detailed methods are provided in the online version of this paper and include the following:

- KEY RESOURCES TABLE
- RESOURCE AVAILABILITY
  - Lead contact
  - Materials availability
  - Data and code availability
- EXPERIMENTAL MODEL AND SUBJECT DETAILS
  - Information about the specimens
- METHOD DETAILS
  - Systematics
  - Electron image and elemental map acquisition
  - Cell size measurements
- QUANTIFICATION AND STATISTICAL ANALYSIS

SUPPLEMENTAL INFORMATION

Supplemental information can be found online at https://doi.org/10.1016/j.cub.2021.03.051.

ACKNOWLEDGMENTS

We acknowledge the facilities and scientific and technical assistance of the Microscopy Australia research facilities at UWA and UNSW. These facilities are funded by the universities and state and commonwealth governments. C. Kong is thanked for his help with electron microscopy and mass spectrometry work. We thank C.T. Baldwin and C. Lenk for field assistance at Loch Torridon and on Eilean Fladday. This resesearch was supported by NERC grant NE/R001324/1 to C.H.W. and P.K.S. and by NASA grant 06-EXOB06-0037 and National Geographic Society grant 8882-11 to P.K.S. and C.H.W. D.W. acknowledges funding from the Australian Research Council via the Future Fellowship Scheme (grant FT140100321).

AUTHOR CONTRIBUTIONS

Original conceptualization was by P.K.S. and M.D.B., with input from C.H.W.; fieldwork was conducted by P.K.S., C.H.W., and M.D.B.; data acquisition and analysis were performed by D.W., M.S., and L.T.; light photomicrography was conducted by P.K.S.; and P.K.S. and C.H.W. wrote the paper, with contributions from D.W. and L.T.

DECLARATION OF INTERESTS

The authors declare no competing interests.

Received: October 14, 2020
Revised: December 7, 2020
Accepted: March 15, 2021
Published: April 13, 2021

REFERENCES

1. Strother, P.K., Battison, L., Brasier, M.D., and Wellman, C.H. (2011). Earth's earliest non-marine eukaryotes. Nature *473*, 505–509.
2. Brasier, A.T., Culwick, T., Battison, L., Callow, R.H.T., and Brasier, M.D. (2017). Evaluating evidence from the Torridonian Supergroup (Scotland, UK) for eukaryotic life on land in the Proterozoic. In Earth System Evolution and Early Life: A Celebration of the Work of Martin Brasier (Special Publications, Volume 448, A.T. Brasier, D. McIlroy, and N. McLoughlin, eds. (Geological Society), pp. 121–144.
3. Strother, P.K., and Wellman, C.H. (2016). Palaeoecology of a billion-year-old non-marine cyanobacterium from the Torridon Group and Nonesuch Formation. Palaeontology *59*, 89–108.
4. Wellman, C.H., and Strother, P.K. (2015). The terrestrial biota prior to the origin of land plants (embryophytes): a review of the evidence. Palaeontology *58*, 601–627.
5. Wacey, D., Saunders, M., Roberts, M., Menon, S., Green, L., Kong, C., Culwick, T., Strother, P., and Brasier, M.D. (2014). Enhanced cellular preservation by clay minerals in 1 billion-year-old lakes. Sci. Rep. *4*, 5841.
6. Wacey, D., Sirantoine, E., Saunders, M., and Strother, P. (2019). 1 billion-year-old cell contents preserved in monazite and xenotime. Sci. Rep. *9*, 9068.
7. Steinberg, M.S. (1975). Adhesion-guided multicellular assembly: a commentary upon the postulates, real and imagined, of the differential adhesion hypothesis, with special attention to computer simulations of cell sorting. J. Theor. Biol. *55*, 431–443.
8. Steinberg, M.S. (2007). Differential adhesion in morphogenesis: a modern view. Curr. Opin. Genet. Dev. *17*, 281–286.
9. Foty, R.A., and Steinberg, M.S. (2005). The differential adhesion hypothesis: a direct evaluation. Dev. Biol. *278*, 255–263.
10. Suga, H., Dacre, M., de Mendoza, A., Shalchian-Tabrizi, K., Manning, G., and Ruiz-Trillo, I. (2012). Genomic survey of premetazoans shows deep conservation of cytoplasmic tyrosine kinases and multiple radiations of receptor tyrosine kinases. Sci. Signal. *5*, ra35.
11. Suga, H., and Ruiz-Trillo, I. (2013). Development of ichthyosporeans sheds light on the origin of metazoan multicellularity. Dev. Biol. *377*, 284–292.
12. Erwin, D.H. (2020). The origin of animal body plans: a view from fossil evidence and the regulatory genome. Development *147*, dev182899.
13. Hehenberger, E., Tikhonenkov, D.V., Kolisko, M., Del Campo, J., Esaulov, A.S., Mylnikov, A.P., and Keeling, P.J. (2017). Novel predators reshape holozoan phylogeny and reveal the presence of a two-component signaling system in the ancestor of animals. Curr. Biol. *27*, 2043–2050.e6.
14. Butterfield, N.J. (2009). Modes of pre-Ediacaran multicellularity. Precambrian Res. *173*, 201–211.
15. Battison, L., and Brasier, M.D. (2012). Remarkably preserved prokaryote and eukaryote microfossils within 1 Ga-old lake phosphates of the Torridon Group, NW Scotland. Precambrian Res. *196–197*, 204–217.
16. Knoll, A.H. (2011). The multiple origins of complex multicellularity. Annu. Rev. Earth Planet. Sci. *39*, 217–239.
17. Xiao, S. (2002). Mitotic topologies and mechanics of Neoproterozoic algae and animal embryos. Paleobiology *28*, 244–250.
18. Thompson, D.W. (1942). On Growth and Form: A New Edition (Cambridge University Press and Macmillan).
19. Forgacs, G., and Newman, S.A. (2005). Biological Physics of the Developing Embryo (Cambridge University Press).
20. Forgacs, G., Foty, R.A., Shafrir, Y., and Steinberg, M.S. (1998). Viscoelastic properties of living embryonic tissues: a quantitative study. Biophys. J. *74*, 2227–2234.
21. Nanjundiah, V. (2016). Cellular slime mold development as a paradigm for the transition from unicellular to multicellular life. In Multicellularity. Origins and Evolution Vienna Series in Theoretical Biology, K.J. Niklas, and S.A. Newman, eds. (MIT Press), pp. 105–130.
22. Sebé-Pedrós, A., Degnan, B.M., and Ruiz-Trillo, I. (2017). The origin of Metazoa: a unicellular perspective. Nat. Rev. Genet. *18*, 498–512.
23. Sebé-Pedrós, A., Irimia, M., Del Campo, J., Parra-Acero, H., Russ, C., Nusbaum, C., Blencowe, B.J., and Ruiz-Trillo, I. (2013). Regulated aggregative multicellularity in a close unicellular relative of metazoa. eLife *2*, e01287.
24. Smith, G.M. (1933). The Freshwater Algae of the United States (McGraw-Hill).
25. Graham, L.E., and Wilcox, L.W. (2000). Algae (Prentice Hall).

26. Chen, L., Xiao, S., Pang, K., Zhou, C., and Yuan, X. (2014). Cell differentiation and germ-soma separation in Ediacaran animal embryo-like fossils. Nature *516*, 238–241.

27. Xiao, S., Muscente, A.D., Chen, L., Zhou, C., Schiffbauer, J.D., Wood, A.D., Polys, N.F., and Yuan, X. (2014). The Weng'an biota and the Ediacaran radiation of multicellular eukaryotes. Natl. Sci. Rev. *1*, 498–520.

28. Xiao, S., Shen, B., Zhou, C., Xie, G., and Yuan, X. (2005). A uniquely preserved Ediacaran fossil with direct evidence for a quilted bodyplan. Proc. Natl. Acad. Sci. USA *102*, 10227–10232.

29. Torruella, G., de Mendoza, A., Grau-Bové, X., Antó, M., Chaplin, M.A., del Campo, J., Eme, L., Pérez-Cordón, G., Whipps, C.M., Nichols, K.M., et al. (2015). Phylogenomics reveals convergent evolution of lifestyles in close relatives of animals and fungi. Curr. Biol. *25*, 2404–2410.

30. Mendoza, L., Taylor, J.W., and Ajello, L. (2002). The class mesomycetozoea: a heterogeneous group of microorganisms at the animal-fungal boundary. Annu. Rev. Microbiol. *56*, 315–344.

31. Yin, Z., Vargas, K., Cunningham, J., Bengtson, S., Zhu, M., Marone, F., and Donoghue, P. (2019). The early Ediacaran *Caveasphaera* foreshadows the evolutionary origin of animal-like embryology. Curr. Biol. *29*, 4307–4314.e2.

32. Cunningham, J.A., Vargas, K., Yin, Z., Bengtson, S., and Donoghue, P.C.J. (2017). The Weng'an Biota (Doushantuo Formation): an Ediacaran window on soft-bodied and multicellular microorganisms. J. Geol. Soc. London *174*, 793–802.

33. Hagadorn, J.W., Xiao, S., Donoghue, P.C.J., Bengtson, S., Gostling, N.J., Pawlowska, M., Raff, E.C., Raff, R.A., Turner, F.R., Chongyu, Y., et al. (2006). Cellular and subcellular structure of neoproterozoic animal embryos. Science *314*, 291–294.

34. Stewart, A.D. (2002). The Later Proterozoic Torridonian Rocks of Scotland (The Geological Society).

35. Glockling, S.L., Marshall, W.L., and Gleason, F.H. (2013). Phylogenetic interpretations and ecological potentials of the Mesomycetozoea (Ichthyosporea). Fungal Ecol. *6*, 237–247.

36. Arroyo, A.S., López-Escardó, D., Kim, E., Ruiz-Trillo, I., and Najle, S.R. (2018). Novel diversity of deeply branching Holomycota and unicellular holozoans revealed by metabarcoding in Middle Paraná River, Argentina. Front. Ecol. Evol. *6*, 99.

37. Parfrey, L.W., Lahr, D.J.G., Knoll, A.H., and Katz, L.A. (2011). Estimating the timing of early eukaryotic diversification with multigene molecular clocks. Proc. Natl. Acad. Sci. USA *108*, 13624–13629.

38. Eme, L., Sharpe, S.C., Brown, M.W., and Roger, A.J. (2014). On the age of eukaryotes: evaluating evidence from fossils and molecular clocks. Cold Spring Harb. Perspect. Biol. *6*, a016139.

39. Fairclough, S.R., Chen, Z., Kramer, E., Zeng, Q., Young, S., Robertson, H.M., Begovic, E., Richter, D.J., Russ, C., Westbrook, M.J., et al. (2013). Premetazoan genome evolution and the regulation of cell differentiation in the choanoflagellate *Salpingoeca rosetta*. Genome Biol. *14*, R15.

40. Richter, D.J., and King, N. (2013). The genomic and cellular foundations of animal origins. Annu. Rev. Genet. *47*, 509–537.

41. Nichols, S.A., Roberts, B.W., Richter, D.J., Fairclough, S.R., and King, N. (2012). Origin of metazoan cadherin diversity and the antiquity of the classical cadherin/β-catenin complex. Proc. Natl. Acad. Sci. USA *109*, 13046–13051.

42. Sebé-Pedrós, A., Roger, A.J., Lang, F.B., King, N., and Ruiz-Trillo, I. (2010). Ancient origin of the integrin-mediated adhesion and signaling machinery. Proc. Natl. Acad. Sci. USA *107*, 10142–10147.

43. Lecuit, T., and Lenne, P.-F. (2007). Cell surface mechanics and the control of cell shape, tissue patterns and morphogenesis. Nat. Rev. Mol. Cell Biol. *8*, 633–644.

44. Zhang, Y., Thomas, G.L., Swat, M., Shirinifard, A., and Glazier, J.A. (2011). Computer simulations of cell sorting due to differential adhesion. PLoS ONE *6*, e24999.

45. Slotznick, S.P., Swanson-Hysell, N.L., and Sperling, E.A. (2018). Oxygenated Mesoproterozoic lake revealed through magnetic mineralogy. Proc. Natl. Acad. Sci. USA *115*, 12938–12943.

46. Jackson, C., Knoll, A.H., Chan, C.X., and Verbruggen, H. (2018). Plastid phylogenomics with broad taxon sampling further elucidates the distinct evolutionary origins and timing of secondary green plastids. Sci. Rep. *8*, 1523.

47. Sánchez-Baracaldo, P., Raven, J.A., Pisani, D., and Knoll, A.H. (2017). Early photosynthetic eukaryotes inhabited low-salinity habitats. Proc. Natl. Acad. Sci. USA *114*, E7737–E7745.

48. Xiao, S., and Tang, Q. (2018). After the boring billion and before the freezing millions: evolutionary patterns and innovations in the Tonian Period. Emerg. Top. Life Sci. *2*, 161–171.

49. Porter, S.M. (2020). Insights into eukaryogenesis from the fossil record. Interface Focus *10*, 20190105.

50. Cole, D.B., Mills, D.B., Erwin, D.H., Sperling, E.A., Porter, S.M., Reinhard, C.T., and Planavsky, N.J. (2020). On the co-evolution of surface oxygen levels and animals. Geobiology *18*, 260–281.

Please cite this article in press as: Strother et al., A possible billion-year-old holozoan with differentiated multicellularity, Current Biology (2021), https://doi.org/10.1016/j.cub.2021.03.051

CellPress
OPEN ACCESS

STAR★METHODS

KEY RESOURCES TABLE

REAGENT or RESOURCE	SOURCE	IDENTIFIER
Biological Samples		
Bicellum brasieri holotype and syntype specimens	This paper	TS09-1
other *B. brasieri* figured specimens	This paper	TS09-2, TOR11-108
dispersed variants of *B. brasieri*	This paper	TOR11-9
milled specimens of *B. brasieri*	This paper	TOR11-108
Software and Algorithms		
Adobe Photoshop	Adobe Systems	CS6

RESOURCE AVAILABILITY

Lead contact

Further information and requests for access to prepared slides and thin sections should be directed to and will be fulfilled by the Lead Contact, Charles Wellman (c.wellman@sheffield.ac.uk).

Materials availability

This study did not generate new unique reagents. Thin sections, including the holotype, along with prepared strew slides, are curated in the palynology collections at the University of Sheffield.

Data and code availability

Data associated with Figures 2H–2J and S3B–S3F are stored in the UWA research repository archive. No codes were generated by this research.

EXPERIMENTAL MODEL AND SUBJECT DETAILS

Information about the specimens

All the specimens of *Bicellum brasieri* mature form (Figure 2) and the variants (Figure 4) illustrated in this report are found embedded in rock thin sections of phosphatic nodules collected by PKS and CHW in 2009 (TS09-1, TS09-2) and in 2011 (TOR11-108) from the Diabaig Formation at the stratotype section at Lower Diabaig, Scotland, UK (Figures 1A–1D). These thin sections are housed in the Palynological Collections at the University of Sheffield, Department of Animal and Plant Sciences, The University of Sheffield, UK. The palynomorphs illustrated in Figure 3 were collected by PKS, CHW and Christopher T. Baldwin from a section of the Diabaig Formation that is exposed on Eilean Fladday immediately opposite the short causeway that when exposed at low tide, gives access to the island from the Isle of Raasay. The sample, TOR11-09 is located 11 m above the base of the section exposure. This material is curated in the Palynological Collections at the University of Sheffield, Department of Animal and Plant Sciences, Sheffield, UK.

METHOD DETAILS

Systematics

A formal systematic description of the taxon, *Bicellum brasieri* Strother & Wellman, gen. et sp. nov. can be found in Data S1, Systematics.

Electron image and elemental map acquisition

Images in Figures 2H, 2I, S3B, and S3C were acquired using a *FEI Helios NanoLab G3 CX* dual beam FIB-SEM instrument using an in lens back-scattered electron detector. The image in Figure S3D was acquired using a *FEI Titan G2 80-200* TEM/STEM in high angle annular dark field (HAADF) mode. Minor image corrections (brightness/contrast) were performed using the open source *ImageJ* software.

The elemental maps presented in Figures 2J, S3E, and S3F were acquired using a *FEI Titan G2 80-200* TEM/STEM with *ChemiSTEM Technology* (Super-X EDX system) operating at 200 kV. Data were acquired from sample wafers of 100-150 nm that were prepared using a *FEI Helios NanoLab G3 CX* dual beam instrument and attached to *Omniprobe* copper TEM holders using platinum connector strips. Multicolored image overlays were performed using the *Gatan Digital Micrograph* software.

Please cite this article in press as: Strother et al., A possible billion-year-old holozoan with differentiated multicellularity, Current Biology (2021), https://doi.org/10.1016/j.cub.2021.03.051

Cell size measurements

Cell size measurements in Tables S1 and S2 were made using the Ruler tool in Photoshop using a scale calibration based on an optical micrometer slide ruled in 10μm intervals.

QUANTIFICATION AND STATISTICAL ANALYSIS

Descriptive statistical data presented in Tables S1 and S2 were calculated in Microsoft Excel based on the size data extracted in Photoshop.